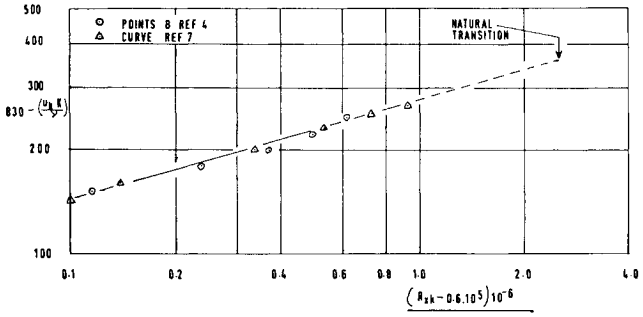

Fig. 5 Correlation for roughness Reynolds number of three-dimensional shapes.

rough guide to the size of the tolerable roughness. Accurate estimates require the specification of another nondimensional group.

For a two-dimensional roughness, the criterion given in Ref. 3 and illustrated in Figs. 2 and 3 is given by

$$826/R_k = 1 + \tfrac{1}{3}\{(2.6\cdot10^6/R_{xk}) - 1\}$$

For a three-dimensional roughness, the experimental results of Tani et al., that are shown in Fig. 3 can be compared with the smooth curve drawn by Tani[7] through the experimental results for the condition when transition is at the roughness element, that is, the values corresponding to point A in Fig. 4. The difference is small because, with an isolated roughness element, transition moves forward very rapidly towards the element. There is evidence that $u_k k/\nu$ tends to a value of about 830 as R_{xk} approaches the value of $0.6\cdot10^5$ that corresponds to the lower stability limit of a laminar boundary layer.[8] A suitable correlation is illustrated in Fig. 5 where the straight line is given by

$$830 - (u_k k/\nu) = 275[(R_{xk} - 0.6\cdot10^5)10^{-6}]^{0.29} \quad (1)$$

If this relation is valid beyond the range of the experimental results used, then with the roughness at the position of natural transition where $R_{xNT} = 2.6\cdot10^6$, the corresponding value of $u_k k/\nu$ tends to 470.

The same results plotted in Fig. 2 fit the relation,

$$R_k = 1300\ (R_{xk}\cdot10^{-6})^{0.15} \quad (2)$$

This equation is simpler than Eq. (1), it is more convenient for design studies, as R_k is based upon the stream velocity, and it agrees with Eq. (1) to within about $\pm2\%$ over the whole range from the instability position to the natural transition position. At the former position it gives an R_k of 850, and at the latter one, of 1500.

6. Comparison of Two-and Three-Dimensional Shapes

There is a difference in the effects of two- and three-dimensional roughness shapes that is of practical interest when a roughness element is close to the starting point of the boundary layer. The present evidence suggests that a two-dimensional cylindrical element can bring transition forward to itself even when the element is at the leading edge, for it is able, by virtue of its drag, to add the necessary ΔR_θ to the boundary layer as well as distorting the boundary-layer profile towards instability conditions. By contrast, it seems that an isolated roughness has a negligible effect upon the momentum thickness of the boundary layer and so, as noted in Ref. 5, it appears to become ineffective when R_{xk} is at or below the value corresponding to the lower limit of stability of the laminar boundary layer.

References

[1] Head, M. R., "Transition Due to Roughness," *Journal of the Royal Aeronautical Society*, Vol. 69, No. 653, May 1965, p. 344.

[2] Dryden, H. L., "Review of Published Data on the Effect of Roughness on Transition from Laminar to Turbulent Flow," *Journal of the Royal Aeronautical Society*, Vol. 20, No. 7, July1953, p. 477.

[3] Gibbings, J. C., "On Boundary-Layer Transition Wires," Current Paper 462, 1959, Aeronautical Research Council.

[4] Tani, I., Komoda, H., and Iuchi, M., "Some Experiments on the Effect of an Isolated Roughness on Boundary-Layer Transition," Rept. 357, 1962, Aeronautical Research Institute.

[5] Klebanoff, P. S., Schubauer, G. B., and Tidstrom, K. D., "Measurements of the Effect of Two-Dimensional and Three-dimensional Roughness Elements on Boundary-Layer Transition," *Journal of the Aeronautical Sciences*, Vol. 22, No. 11, Nov. 1955, p. 803–804.

[6] Gazely, C., Jr., "Boundary-Layer Stability and Transition in Subsonic and Supersonic Flow," *Journal of the Aeronautical Sciences*, Vol. 20, No. 1, Jan. 1953, p. 19.

[7] Tani, I., "Effect of Two-Dimensional and Isolated Roughness on Laminar Flow," *Boundary Layer and Flow Control*, edited by G. V. Lachman, Pergamon, 1961, p. 637.

[8] Schlichting, H., *Boundary Layer Theory*, 4th ed. McGraw-Hill, New York, 1960, p. 397.

Thin Airfoil in Nonuniform Parallel Streams

L. Ting* and C. H. Liu†
New York University, Bronx, N. Y.

1. Introduction

THE small disturbance theory for two parallel streams was initiated by von Kármán.[1] The undisturbed streams with velocity U_1 and U_2 are separated by the streamline represented by the x axis. A thin airfoil represented by a single vortex of strength Γ was located as in the lower stream with velocity U_1 at a distance d below the origin. According to the small disturbance theory, the condition of matching pressure $U_1u'_1 = U_2u'_2$ and that of matching slope $v'_1/U_1 = v'_2/U_2$ are imposed along the undisturbed streamline, the x axis. These boundary conditions are fulfilled by the introduction of images.[1] The disturbance velocity potential for the lower stream is

$$w_1(z) = \Gamma/(2\pi i)\ln(z + di) + \lambda_1\Gamma/(2\pi i)\ln(z - di) \quad (1)$$

where $z = x + iy$ and $\lambda_1 = (U_1^2 - U_2^2)/(U_1^2 + U_2^2)$. The second term represented the reflected image located at $z = di$ with strength $\lambda_1\Gamma$. The disturbance velocity potential for the upper stream is

$$w_2(z) = \Gamma\lambda_2/(2\pi i)\ln(z + di) \quad (2)$$

It represents the "diffracted" disturbance with $\lambda_2 = 2U_1U_2/(U_1^2 + U_2^2)$. It should be noted that $|\lambda_1|$ is less than unity and is equal to unity only in the two limiting cases: 1) $U_2/U_1 = 0$, $\lambda_1 = 1$, and line $y = 0$ is a constant pressure free streamline and 2) $U_2/U_1 \to \infty$, $\lambda_1 = -1$, and line $y = 0$ represents a solid wall. Extensions of the method of images to a flowfield of three parallel streams, i.e., two dividing streamlines as shown in Fig. 1, have been made[2] for the special case of jets ($U_1 = U_3 = 0$) and wakes ($U_1 = U_3 \neq U^2$). In this Note, a system of images will be formulated for the general case $U_1 \neq U_2 \neq U_3$ and the airfoil will be represented by a vorticity distribution. The distribution will be determined in a similar manner for an airfoil in a uniform

Received July 22, 1968. This work was supported by Army Research Office, Durham, Contract DA-31-124-ARO-D-464.

* Professor of Aeronautics & Astronautics. Member AIAA.

† Research Assistant, Aerospace Laboratory.

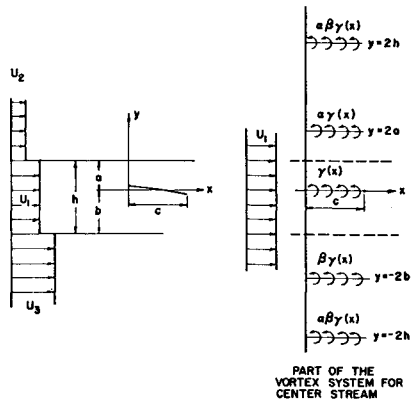

Fig. 1 Thin airfoil in the center stream of three parallel ones.

stream. Numerical results are obtained for the special case when one of the dividing streamlines is a solid wall.

2. Analysis

Figure 1 shows three parallel streams with velocity U_2, U_1, and U_3. For the analysis of the aerodynamic forces on the airfoil, it is necessary only to construct the disturbance velocity potential at the stream where the airfoil is located.

If a vortex is located at the origin and is in the center stream, the upper dividing streamline is $y = a$ and the lower streamline is $y = -b$. The reflected image with respect to these two lines are $\alpha\Gamma$ at $z = 2ai$ and $\beta\Gamma$ at $z = -2bi$ with $\alpha = (U_1^2 - U_2^2)/(U_1^2 + U_2^2)$ and $\beta = (U_1^2 - U_3^2)/(U_1^2 + U_3^2)$. The reflections of these two images with respect to the opposite dividing streamlines are $\alpha\beta\Gamma$ at $z = -2(a + b)i$ and $\beta\alpha\Gamma$ at $z = 2(a + b)i$. By the method of successive reflections, the disturbance potential for the central layer due to a single vortex at the origin is

$$w_1 = \frac{\Gamma}{(2\pi i)}\left\{\ln z + \sum_{j=0,1,2,\ldots} (\alpha\beta)^j[\alpha \ln(z - 2jhi - 2ai) + \beta \ln(z + 2jhi + 2bi) + \alpha\beta \ln(z^2 + 4(j+1)^2h^2)]\right\} \quad (3)$$

where $h = a + b$.

A thin airfoil with chord length C lying in the middle stream can be represented by a distribution of vortex with density $\gamma(x)$ along the x axis from the origin to $x = C$, as shown in Fig. 1. Each vortex element $\gamma(x)\,dx$ will form a system of images as described by Eq. (3). The distribution $\gamma(x)$ will then be determined by the linearized boundary condition along the airfoil, i.e.,

$$v(x, 0)/U_1 = m(x) - \alpha \quad (4)$$

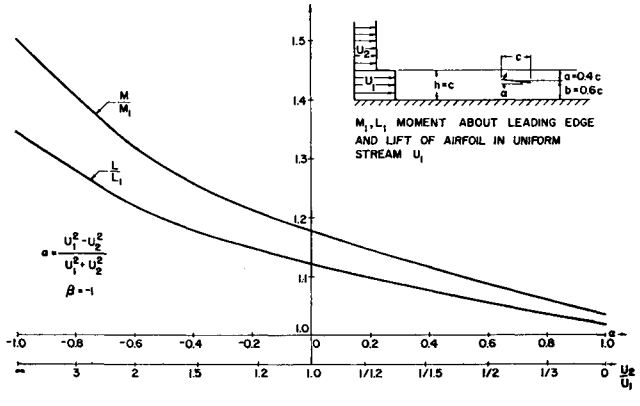

Fig. 2 Change of lift and moment due to nonuniform stream and wall effect.

where α is the angle of attack, $m(x)$ is the slope of the mean camber line at zero angle of attack, and $v(x, 0)$ is the vertical velocity induced by the vortex distribution $\gamma(x)$ and its system of images. From Eq. (3), it is obtained

$$v(x,0) = \frac{1}{2\pi}\int_0^C \left\{\frac{1}{x - x'} + \sum_{j=0,1,2,\ldots} (\alpha\beta)^j\left[\frac{\alpha(x - x')}{(x - x')^2 + 4(jh + a)^2} + \frac{\beta(x - x')}{(x - x')^2 + 4(jh + b)^2} + \frac{2\alpha\beta(x - x')}{(x - x')^2 + 4(j + 1)^2h^2}\right]\right\} \times \gamma(x')dx' \quad (5)$$

Equations (4) and (5) form the integral equation for $\gamma(x)$ subjected to the Kutta-Joukowski condition $\gamma(C) = 0$. The first term of the kernel is singular and is the same as that for the classical problem of an airfoil in a uniform stream. By following the classical approach,[3] new variables θ and φ will be introduced with $x = \frac{1}{2}C(1 - \cos\varphi)$ and $x' = \frac{1}{2}C(1 - \cos\theta)$, and $\gamma(x)$ will be expressed as a series in φ,

$$\gamma(x) = 2U_1\left\{A_0 \cot\frac{\varphi}{2} + \sum_{M=1,2,\ldots} A_M \sin M\varphi\right\} \quad (6)$$

where $A_0, A_1, A_2, \ldots$ are unknown constants. Equations (4) and (5) become

$$\left\{A_0 - \sum_{M=1,2,\ldots} A_M \cos M\varphi\right\} + \sum_{M=0,1,2,\ldots}\sum_{j=0,1,2,\ldots}\sum_{k=1,2}^{3} \{A_M J_M(j,k,\varphi)(\alpha\beta)^j F_k\} = d_0 + \sum_{M=1,2,\ldots} d_M \cos M\varphi \quad (7)$$

d_0 and d_M are the cosine Fourier coefficients of the given function $m(x) - \alpha$. The terms in the curly brackets are the terms in the classical problem. The three F_k's are α, β, and $\alpha\beta$, respectively, for $k = 1, 2, 3$. The functions, $J_M(j, k, \varphi)$'s are defined as

$$J_0 = \frac{1}{\pi}\int_0^\pi \frac{(\cos\theta - \cos\varphi)\sin\theta}{(\cos\theta - \cos\varphi)^2 + Y_{jk}^2} \cot\frac{\theta}{2}\,d\theta$$

and

$$J_M = \frac{1}{\pi}\int_0^\pi \frac{(\cos\theta - \cos\varphi)\sin\theta}{(\cos\theta - \cos\varphi)^2 + Y_{jk}^2} \sin M\theta\, d\theta \quad \text{for } M = 1, 2, \ldots$$

where $Y_{jk} = 4(jh + e_k)/C$ with $e_1 = a$, $e_2 = b$, and $e_3 = a + b$. These integrals are carried out by contour integration in Ref. 4. The result is

$$J_0 = [2(R - R^{-1})\cos\delta + R^2 - \cos 2\delta]/[R^2 + R^{-2} - 2\cos 2\delta]$$

$$J_M = -R^M \cos M\delta \qquad \text{for } M = 1, 2, \ldots$$

where

$$R = 2^{1/2}/\{[2 + Z + (Z^2 + 4Y^2)^{1/2}]^{1/2} + [Z + (Z^2 + 4Y^2)^{1/2}]^{1/2}\}$$

$$0 \le \delta = \arccos(\cos\varphi\{2/[2 + Z + (Z^2 + 4Y^2)^{1/2}]\}) \le \pi$$

$$Z = Y^2 - \sin^2\varphi$$

and Y stands for Y_{jk}. The left side of Eq. (7) can be resolved into cosine Fourier series in φ, and by equating the coefficients on both sides of Eq. (7), a set of algebraic equations for the unknown $A_0, A_1, \ldots$ are obtained

$$\sum_{L=0,1,\ldots} B_{OL}A_L = \pi d_0, \quad \sum_{L=0,1,\ldots} B_{ML}A_L = \frac{\pi d_M}{2} \quad \text{for } M = 1, 2, \ldots \quad (8)$$

with

$$B_{ML} = \sum_{j=0,1,\ldots} \sum_{k=1,2}^{3} (\alpha\beta)^j F_k \int_0^\pi J_L(j,k,\varphi) \cos M\varphi \, d\varphi \quad (9)$$

The coefficients B_{ML} can be evaluated by numerical integration for a finite number of images. When $\gamma(x)$ is represented by a finite Fourier series, the algebraic equations for A_M can be solved. A numerical program for the computations is presented in Ref. 4. Figure 2 shows the changes in lift and in moment about leading edge of a flat plate due to nonuniform streams. With $\beta = -1$, $U_3/U_1 = \infty$, the lower dividing streamline is a solid wall. When α decreases from 1 to 0 to -1, U_2/U_1 increases from 0 to 1 to ∞, and both lift and moment increase. At $\alpha = 0$, the airfoil is in a wall jet of thickness $h = a + b = C$. At $\alpha = 1$, the airfoil is in a semi-infinite uniform stream near the wall. At $\alpha = -1$, the airfoil is in a uniform stream between two parallel walls.

If the airfoil is located in one of the outer streams, say the upper stream, it is necessary to reconstruct the system of images for a single vortex located at the origin and lying in the upper stream. The locations of the two dividing streamlines will be $y = -a$ and $y = -b$, respectively, with $h = b - a > 0$. The disturbances potential in the upper stream is shown in Ref. 4 to be represented by the following vortex system:

$$w_2 = \frac{\Gamma}{(2\pi i)} \left\{ \ln z - \alpha \ln(z + 2ai) + \alpha^2\beta \sum_{j=0,1,\ldots} (\alpha\beta)^j \ln[z - 2(j+1)hi] \right\} \quad (10)$$

where $\alpha = 2U_1U_2/(U_1^2 + U_2^2)$. With Eq. (3) replaced by Eq. (10), the preceding procedure can be repeated to compute the flowfield for an airfoil in one of the outer streams.

3. Concluding Remarks

By repeatedly applying the method of images across a streamline dividing two parallel streams of unequal velocities, the linearized theory for a thin airfoil in three parallel streams is completed. The same procedure can be extended to larger numbers of parallel streams. The linearized theory for an airfoil with jet flap can also be extended to include the effects of nonuniform streams. Since the method of images applies also to the doublets distributions, solutions for an airfoil with finite thickness and camber in parallel streams can also be constructed so long as the dividing streamlines are disturbed slightly. These extensions will be reported later.

It should also be pointed out, when none of the dividing streamlines represent a rigid wall, the resultant effect of the vortex and the images will not cancel out at far upstream and downstream, and the vertical displacement of the dividing streamlines relative to the position at $x = 0$ will be infinite. When the vertical positions of the airfoil relative to the dividing streamlines in its neighborhood ($x \sim 0$) are specified, the linearized solution presented in this Note is valid locally and is, in general, not uniformly valid at large distances. On the other hand, when the vertical positions of the airfoil relative to the dividing streamlines far upstream are specified, the present linearized solution is not immediately applicable since a matching outer solution is not yet available. However, for the special case when one of the dividing streamlines represents a rigid wall, the vertical displacement of all the streamlines will be small uniformly and the linearized solution is uniformly valid with the classical exception of the neighborhood of the leading edge. The numerical examples of this Note belongs to this special case.

References

[1] von Kármán, Th., "Beitrag zur Theorie des Auftirebes," *Vortraege aus dem Gebiete der Aerodynamik und verwandter Gebiete*, Springer-Verlag, Aachen, 1929, pp. 95–100.

[2] Glauert, H., "Influence of a Uniform Jet in the Lift of an Airfoil," R&M 1478, 1932, Aeronautical Research Council, London.

[3] Glauert, H., *The Elements of Aerofoil and Airscrew Theory*, 2nd ed., Cambridge University Press, London, 1947.

[4] Ting, L. and Liu, C. H., "Thin Airfoil in Non-Uniform Parallel Streams," Rept. AA 68-20, July 1968, New York Univ.